

## Sensory and Motor Systems

# Off Starburst Amacrine Cells in the Retina Trigger Looming-Evoked Fear Responses in Mice

Jeremy M. Bohl,<sup>1,\*</sup> Jui Gope,<sup>1,2,\*</sup> Zachary J. Sharpe,<sup>1,\*</sup> Angela Shehu,<sup>1</sup> Andrew Garrett,<sup>1,3</sup> Christina C. Koehler,<sup>1</sup> Chase B. Hellmer,<sup>1</sup> and Tomomi Ichinose<sup>1</sup>

<https://doi.org/10.1523/ENEURO.0183-22.2023>

<sup>1</sup>Department of Ophthalmology, Visual and Anatomical Sciences, Wayne State University School of Medicine, Detroit, MI 48201, <sup>2</sup>Department of Public Health, Wayne State University School of Medicine, Detroit, MI 48201, and <sup>3</sup>Department of Pharmacology, Wayne State University School of Medicine, Detroit, MI 48201

## Abstract

A rapidly approaching dark object evokes an evolutionarily conserved fear response in both vertebrates and invertebrates, young to old. A looming visual stimulus mimics an approaching object and triggers a similarly robust fear response in mice, resulting in freeze and flight. However, the retinal neural pathway responsible for this innate response has not been fully understood. We first explored a variety of visual stimuli that reliably induced these innate responses, and found that a looming stimulus with 2-d acclimation consistently evoked fear responses. Because the fear responses were triggered by the looming stimulus with moving edges, but not by a screen flipping from light to dark, we targeted the starburst amacrine cells (SACs), crucial neurons for retinal motion detection. We used intraocular injection of diphtheria toxin (DT) in mutant mice expressing diphtheria toxin receptors (DTR) in SACs. The looming-evoked fear responses disappeared in half of the DT-injected mice, and the other mice still exhibited the fear responses. The optomotor responses (OMRs) were reduced or eliminated, which occurred independent of the disappearance of the fear responses. A histologic examination revealed that ON SACs were reduced in both mouse groups preserved or absent fear responses. In contrast, the number of OFF SACs was different among two groups. The OFF SACs were relatively preserved in mice exhibiting continued fear responses, whereas they were ablated in mice lacking fear response to looming stimulation. These results indicate that OFF SACs and the direction-selective pathway in the retina play a role in looming-induced fear behaviors.

**Key words:** fear response; flight; looming stimulus; starburst amacrine cell; vision test

## Significance Statement

In response to a suddenly approaching dark object, mice exhibit a defensive response: either flight to a refuge or freeze in the same spot. How the visual system evokes this response in the mouse has not been fully understood. We focused on the initial neural component of the visual system, the retina, and examined a type of neuron known for sensing object motion: the starburst amacrine cell (SAC). We found that ablation of OFF starburst amacrine cells removed the dark object-evoked defensive responses. We believe that our findings will contribute to understanding the neural network connecting the visual system and the brain circuit regarding fear and emotion.

## Introduction

The fear response to an approaching predator is a crucial innate behavior for survival. The looming object-

evoked fear response occurs in many species of vertebrates and invertebrates that are equipped with visual systems, including locusts, flies, fish, rodents, and humans from infancy

Received May 6, 2022; accepted February 18, 2023; First published April 3, 2023.

The authors declare no competing financial interests.

Author contributions: J.G., C.C.K., C.B.H., and T.I. designed research; J.M.B., J.G., Z.J.S., A.S., A.G., C.C.K., C.B.H., and T.I. performed research; J.M.B., J.G., Z.J.S., A.S., and T.I. analyzed data; J.M.B., Z.J.S., A.S., and T.I. wrote the paper.

to adulthood (Schiff et al., 1962; Blanchard et al., 2001, 2002; Yilmaz and Meister, 2013; Temizer et al., 2015; Klapoetke et al., 2017; Bertels et al., 2020). The looming stimulus consists of an expanding dark circle above the head that robustly induces fear responses in mice (Yilmaz and Meister, 2013; De Franceschi et al., 2016; Koehler et al., 2019). Flight (dash to a refuge) or freezing is commonly observed in response to the looming stimulus, although a diversity of responses among mice is documented (Yilmaz and Meister, 2013; De Franceschi et al., 2016; X. Yang et al., 2020).

Neural networks responsible for the looming behavior have been investigated in the central nervous system (Mobbs et al., 2009; J. Yang et al., 2012; Ren and Tao, 2020); however, looming stimulus-sensing retinal neural circuits have not been fully understood. In the mouse retina, visual signals are captured by photoreceptors and transferred to ~15 types of bipolar cells (Euler et al., 2014; Ichinose et al., 2014; Ichinose and Hellmer, 2016; Shekhar et al., 2016), which relay differing visual features to 60 types of amacrine cells (Yan et al., 2020) and 50 types of ganglion cells (Baden et al., 2016). Most retinal neurons can be further categorized as ON or OFF types, which respond to light or dark objects, respectively. Because an expanding dark spot with moving edges uniquely evokes fear responses, the OFF channel of direction-selective cells in the retina are expected to contribute predominantly to looming-evoked behavior (Yilmaz and Meister, 2013).

Two types of OFF cell pathways have been shown to convey looming-evoked fear responses. The PV-5 OFF ganglion cells are sensitive to approaching motion (Münch et al., 2009). Also, a neural pathway of vGluT3 amacrine cells, W3 and OFF t- $\alpha$  ganglion cells mediate the looming-evoked defensive responses (Kim et al., 2020; Wang et al., 2021). The latter pathway is critical for sensing local motion, and the ablation of these neurons eliminates the defensive responses to looming stimuli (Kim et al., 2020; Wang et al., 2021). However, there might be other mechanisms in the retinal network, similar to those found in the fly and locust visual system (Gabbiani et al., 2002; Klapoetke et al., 2017). The direction-selective pathway (Yoshida et al., 2001; Euler et al., 2002), may sense the looming stimulus as a dark moving edge.

To investigate whether the direction-selective pathway in the retina contributes to looming detection, we ablated starburst amacrine cells (SACs) using an intraocular injection of diphtheria toxin (DT). Looming stimulus-evoked behaviors and the optomotor responses (OMRs) were

monitored before and after the SAC ablation. We found that OFF SACs and the direction-selective pathway are critical components for looming-induced fear responses.

## Materials and Methods

### Ethical approval

All animal purchasing, handling and procedures were approved by the Institutional Animal Care and Use Committee at Wayne State University School of Medicine. All the necessary steps were taken to minimize animal suffering and all experimentation was conducted in accordance with relevant guidelines and regulations. The tissues were harvested immediately after the animals were euthanized by CO<sub>2</sub> inhalation and cervical dislocation.

### Animals

Transgenic mice expressing Cre recombinase in SACs (ChAT-Cre, stock #031661, The Jackson Laboratory, RRID: [IMSR\\_JAX:031661](#)) were crossed with a mouse line containing the diphtheria toxin receptor, the expression of which can be induced by Cre-mediated recombination (ROSA-iDTR, stock #007900, The Jackson Laboratory, RRID: [IMSR\\_JAX:007900](#)). Control mice were of the C57BL/6J strain (stock #000664, The Jackson Laboratory, RRID: [IMSR\\_JAX:000664](#)). Mice were maintained in group cages separated by sex; both males and females were used in the study. Mice were provided with food and water *ad libitum* and maintained on a 12/12 h light/dark cycle.

### Visual testing

The methods of visual stimulation and mouse handling were based on the procedures described previously (Yilmaz and Meister, 2013; De Franceschi et al., 2016; Koehler et al., 2019). In brief, the testing arena consisted of a 40 × 50 × 33 cm (width × length × height) enclosure with an overhead computer monitor for stimulus display and a plastic hut to serve as a shelter. The arena was held at a mesopic light level of 7 × 10<sup>5</sup> photons/μm<sup>2</sup>/s before visual stimulation. Stimuli were generated in MATLAB (MathWorks, RRID: [SCR\\_001622](#)) using PsychToolbox3 (RRID: [SCR\\_002881](#)). The day before testing, each mouse was given 10 min to acclimate to the testing arena and become familiar with the location of the shelter. On testing day, mice were given another 10 min to acclimate to the arena before stimulus onset. When a mouse was at least 500 mm from the shelter, a visual stimulus was presented. The mouse's movement during each trial was video captured using a CCD camera (Ultrasensitive CCD, Teledyne Lumenera) with associated recording software (Stream Pix 7, NorPix, RRID: [SCR\\_015773](#)). Each mouse received only one trial of the looming stimulus in a given day.

Each mouse was tested with one of the three stimuli: looming, receding circle, or flip screen. The primary looming stimulus was a 2° black disk that rapidly expanded until it reached 50° within 250 ms on a gray background (Fig. 1Aa). In some cases, the looming stimulus expanded from 2° to 9°. Mice were tested with either a single looming stimulus or a looming stimulus that repeated 10 times (1-time or 10-time). The receding white circle stimulus

This work was supported by an Undergraduate Research Opportunity (UROP) grant (J.G.), National Institutes of Health (NIH) Project Grants R01 EY028915 and EY032917 (to T.I.), co-financed by Research to Prevent Blindness (RPB), and the Rumble Fellowship by the Wayne State University Graduate School (C.B.H.).

\*J.M.B., J.G., and Z.J.S. contributed equally to this work.

Correspondence should be addressed to Tomomi Ichinose at [tichinos@med.wayne.edu](mailto:tichinos@med.wayne.edu).

<https://doi.org/10.1523/ENEURO.0183-22.2023>

Copyright © 2023 Bohl et al.

This is an open-access article distributed under the terms of the [Creative Commons Attribution 4.0 International license](#), which permits unrestricted use, distribution and reproduction in any medium provided that the original work is properly attributed.

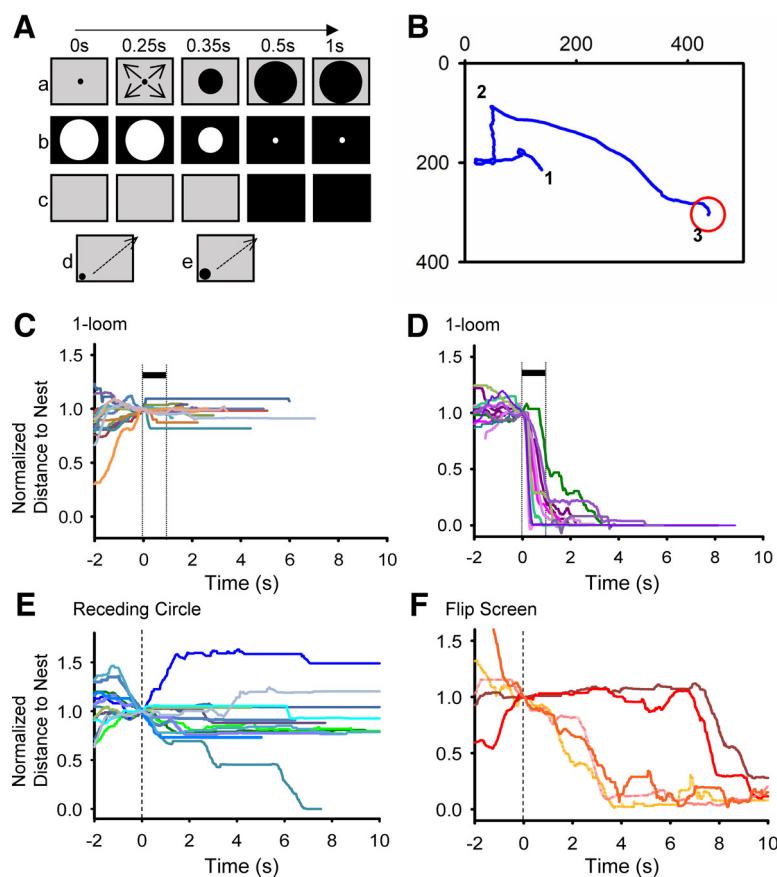


**Figure 1.** Visual stimuli and mouse behavior. **A**, Visual stimuli we tested: **a**, looming stimulus; **b**, white receding stimulus; **c**, flip screen stimulus; **d**, sweeping stimulus; **e**, large sweeping stimulus. **B**, A sample mouse track record. A mouse was placed in an arena of  $400 \times 500$  mm with a hut for the mouse to escape from the stimulus (red circle). After 10-min acclimation, video capturing started (1), a looming stimulus started (2), and the mouse came into the shelter (3). **C**, Based on the mouse tracking records, the distance to the nest over the time was calculated and plotted. After normalization to the distance at the stimulus onset (time = 0 s), the distances for individual mice were plotted before and after the 1-time looming stimuli. A dark bar indicates the timing of the 1-looming stimulus. The vertical dashed line at time 0 s indicates stimulus onset. The 1.0 indicates the position when the visual stimulus started, while the location of the shelter was 0. A group of mice froze to the stimuli (14/26 mice). Each line color indicates the track of each mouse. **D**, The same stimulus evoked immediate flight responses to another group of mice (12/26 mice). **E**, 10-time receding white circle evoked freeze responses in 13/25 mice. **F**, Flip screen did not evoke fear responses (6 mice).

consisted of a large white circle receding to a small dot on a black background (Fig. 1*Ab*). The flip screen stimulus changed from a gray background to a dark background instantaneously (Fig. 1*Ac*). The sweeping circle stimulus (De Franceschi et al., 2016) was used to simulate a predator searching for prey. Two sizes were used: a smaller black disk that made a  $5.7^\circ$  visual angle size to a mouse in the arena, and a larger  $8.5^\circ$  black disk, both at a speed of  $21^\circ$  per second (Fig. 1*Ad,e*).

### Optomotor response (OMR) and slow-angled descent forepaw grasping (SLAG) test

Optomotor response (OMR) testing was used to assess each mouse's visual contrast sensitivity before and after diphtheria toxin injection using the Optodrum system (Striatech). The walls of the square testing arena consist of four computer screens. In the center of the arena, a mouse is placed on an elevated stage. The mouse sits unrestricted on the stage as the walls project a rotating

black and white striped stimulus that triggers the OMR. A camera at the top of the Optodrum tracks the mouse's head movements. The contrast sensitivity was measured at a spatial frequency of 0.064 cycles/degree. The presence or absence of optomotor tracking was automatically tracked by the included software package which analyzes the correlation between the angular velocities of the mouse's head and the rotation of the stimulus. Mice were tested at a variety of contrast levels set automatically by the software's staircase algorithm, which was provided by the system (Striatech), and used by Prusky et al. (2004), which determined the step size between contrast levels. Clockwise and counterclockwise stimuli were used to determine optomotor reflexes driven by the left and right eyes, respectively (Prusky et al., 2004; Douglas et al., 2005). Testing of a combined control/experimental group was performed using a single blind method where groups were mixed together and referred to by a temporary identifier with the condition unknown to the experimenter. Contrast thresholds obtained in OMR testing

were converted to contrast sensitivities by calculating their reciprocal.

Mice were tested for functional vision after DT injection using the slow-angled descent forepaw grasping (SLAG) test (Gil-Pages et al., 2013). Mice held by the tail were lowered over a wire cage lid until they were several centimeters away from the edge. A mouse with functional vision will reach toward the cage in an attempt to grasp it. The procedure is repeated with the mouse facing away from the lid of the cage, and a mouse with functional vision will twist to reach toward the lid. Videos were recorded and scored by two experimenters.

### Intraocular diphtheria toxin injection

Procedures regarding the diphtheria toxin injection timing and concentration followed the method previously described (Hillier et al., 2017; Kim et al., 2020). Mice were anesthetized for intraocular injection using a mixture of ketamine (80  $\mu\text{g}/\text{kg}$ ) and xylazine (5  $\mu\text{g}/\text{kg}$ ). Glass micropipettes for injection were prepared using a P1000 micropipette puller (Sutter Instruments). Injection was performed using a Nanoject III precision pipette (Drummond Scientific). DT (D0564, Millipore Sigma) was diluted to a working concentration of 0.8 ng/ $\mu\text{l}$ , and 2  $\mu\text{l}$  was injected into the intravitreal space of each eye twice, 48 h apart. For some mice, 2  $\mu\text{l}$  DT solution at a concentration of 5 ng/ $\mu\text{l}$  was injected to the intravitreal space only once. Subsequent behavioral and cellular experiments were conducted 6–10 d after the initial DT injection. Control mice were injected with 0.9% normal saline in both eyes on the same schedule as toxin-injected mice.

### Immunostaining and imaging

Detailed methods for the mouse dissection and our standard immunostaining procedures are described in our previous publication (Ichinose et al., 2014; Farshi et al., 2016). In brief, eyes were enucleated immediately after euthanasia with  $\text{CO}_2$  gas and cervical dislocation, and were transferred to a dissection chamber with oxygenated HEPES buffer solution composed of the following (in mM): 115 NaCl, 2.5 KCl, 2.5  $\text{CaCl}_2$ , 1.0  $\text{MgCl}_2$ , 10 HEPES, and 28 glucose, adjusted to pH 7.37 with NaOH. Retinal tissue was isolated, and mounted on a piece of nitrocellulose filter paper. Retinal tissue on the filter paper was fixed for 60 min in 4% paraformaldehyde in 0.1 M phosphate buffer (PB). Tissue was blocked for 60 min in 10% normal donkey serum (NDS) dissolved in 0.5% Triton X-100 in 0.01 M PBS (PBS-T). Primary antibody goat anti-choline acetyltransferase (ChAT-antibody, Millipore Sigma catalog #AB144P, RRID: AB\_2079751) at 1:200 concentration was dissolved in 3% NDS in PBS-T and incubated overnight at room temperature. The secondary antibody was Donkey Anti-Goat Alexa 568 (Thermo Fisher Scientific catalog #A-11057, RRID: AB\_2534104) or Donkey Anti-Goat Alexa 633 (Invitrogen catalog #A31083, RRID: AB\_2535739) at 1:500 concentration for 2 h; 1  $\mu\text{M}$  4',6'-diamino-2-phenylindole (DAPI) in 3% NDS in PBS-T was added for 15 min at room temperature. Tissue was washed and mounted for imaging with a confocal microscope (TCS SP8, Leica).

### Data analysis and statistics

Video files generated during stimulus testing were analyzed as follows; the location of the mouse's nose in each frame was manually tracked using software (Image Pro Plus, RRID: SCR\_016879, Media Cybernetics), which returned the x and y coordinates in the arena versus time. The video images were skewed, which were corrected, accordingly (Koehler et al., 2019). The speed of the mouse's movement was calculated based on the x-y location differences between two frames. The maximum speed was the highest speed measured during the actual flight or escape response.

Mouse response to a visual stimulus was separated into three categories based on previous publications (De Franceschi et al., 2016; Koehler et al., 2019). Flight: a mouse dashed to the shelter with the following three criteria: (1) the speed was at least 300 mm/s; (2) the flight speed reached its maximum within 0.5 s; and (3) the mouse directly went into the nest or next to it after the initial flight response. Freeze: a mouse remained immobilized for >1 s at a speed of 0 mm/s, accompanied by no movement of the head or tail. Rearing: a mouse stood up on hind legs and observed the visual stimulus.

Cell counting was conducted using peripheral retinal tissue. One randomly selected 290  $\times$  290  $\mu\text{m}$  field per tissue with step size of 1  $\mu\text{m}$  was captured to image DAPI stained cells in the ganglion cell layer (GCL). Alexa-633-labeled ON and OFF SACs were similarly imaged in the GCL and inner nuclear layer (INL), respectively. Confocal image stacks were subjected to three-dimensional deconvolution using the AutoQuant X3 platform (Media Cybernetics, RRID: SCR\_002465). Cell counting of SACs was performed manually using both a cell counter plugin available with the Fiji distribution of the NIH ImageJ platform (Schindelin et al., 2012; RRID: SCR\_002285) or a manual cell counter overlay available in the aforementioned LAS X software. Counting of the much more numerous DAPI-stained cells was performed using an AIVIA3D Object Analysis-Meshes recipe from Leica and DRVISION (Bellevue).

Statistical analysis was performed in Microsoft Excel (Microsoft; RRID: SCR\_016137) and GraphPad Prism (GraphPad Software; RRID: SCR\_002798). Either an unpaired Student's *t* test or one-way ANOVA with *post hoc* analysis was used to compare multiple groups.

### Results

The looming stimulus evokes fear responses in mice, including freeze and flight (Yilmaz and Meister, 2013; De Franceschi et al., 2016). Cellular and molecular mechanisms for looming stimulus detection and fear responses have not been fully understood. In the current study, we focused on the direction-selective pathway in the retina to explore its contribution to visually-evoked fear behaviors.

### Wild-type mice exhibited fear responses to visual stimuli

A C57 wild-type mouse was placed in a behavior arena, and a looming stimulus was activated on a monitor placed



**Table 1: The various visual stimuli-evoked behavioral responses in C57 wild-type (WT) mice**

| C57 WT             | Mouse number | Flight    | Freeze   | Rearing  | No response |
|--------------------|--------------|-----------|----------|----------|-------------|
| 1-looming          | 26           | 12 (46%)  | 14 (53%) | 0        | 0           |
| 10-looming         | 39           | 39 (100%) | 18 (46%) | 5 (13%)  | 0           |
| 10-loom (no accl*) | 13           | 2 (15%)   | 2 (15%)  | 9 (69%)  | 1 (8%)      |
| Flip screen        | 6            | 0         | 0        | 2 (33%)  | 4 (66%)     |
| White receding     | 25           | 2 (8%)    | 13 (52%) | 13 (52%) | 2 (8%)      |
| Sweep (small)      | 18           | 0         | 7 (39%)  | 8 (44%)  | 4 (22%)     |
| Sweep (large)      | 17           | 0         | 9 (53%)  | 1 (6%)   | 7 (41%)     |

Some mice showed multiple responses to a stimulus, such as freezing followed by flight. Therefore, the totals exceed 100% for some stimuli. \*no accl: acclimation was not conducted the day before the experiment.

on the ceiling of the arena (Fig. 1Aa; Koehler et al., 2019). The mouse was allowed to move freely in the arena (Fig. 1B point 1 to 2). A visual stimulus was initiated when a mouse was located in the middle of the arena and away from the shelter (red circle). If a looming stimulus was projected, the mouse quickly moved into the shelter, displaying a flight response (Fig. 1B point 2 to 3). The mouse's movement was tracked and the distance to the shelter from each point was plotted as a function of time before and after visual stimulation. Figure 1C–F shows the distance from the nest after being normalized to position at stimulus onset. Each mouse was acclimated a day before and on the day of the looming experiment, which induced robust fear responses during the looming stimulus (see later for more detail).

We evaluated the impact of several stimulus parameters on the evocation of fear responses. The one-time looming stimulus evoked either a freeze (Fig. 1C) or flight response (Fig. 1D). The probability of displaying either response was about half (Table 1). We also aimed to examine whether the direction of the darkening is crucial. We presented a group of mice with a white receding circle, which darkened the monitor from the periphery instead of the center (Fig. 1Ab). The white receding circle evoked freeze responses in about half of the mice we tested (Table 1; Fig. 1E). Mice also exhibited either flight (8%), rearing (52%), or a combination of these. The rearing response indicates weak threat-elicited behavior (X. Yang et al., 2020), thus, the white receding circle is considered to be a weak threat stimulus.

We wondered whether the darkening of the arena causes the fear responses in mice. We applied a stimulus consisting of the screen flipping from gray to dark without a moving dark edge (Fig. 1Ac). Two mice showed rearing (33%; Table 1), but none showed freeze or flight responses (Fig. 1F). These results suggest that a moving dark edge is crucial to cause the fear-evoked freeze and flight responses.

Another study (De Franceschi et al., 2016) previously showed that a sweeping dark circle evoked freeze responses in 84% of mice, whereas the looming stimulus evoked flight responses. We then conducted a sweeping dark circle stimuli of 5.7° (Fig. 1Ad). In our study, however, the sweeping stimulus evoked a freeze in only 39% of mice (Table 1). We increased the size of the sweeping circle to 8.5° (Fig. 1Ae), which evoked a freeze 53% of mice, slightly increased from the smaller stimulus (Table 1). Mice in our colony did not consistently exhibit fear-

based flight or freeze in response to the sweeping stimulus.

To evoke fear responses more consistently, we exposed the mice to a 10-time repeating looming stimulus. All mice exhibited flight response (Table 1). Some of them froze first, then dashed to the shelter (flight response; Fig. 2A; Table 1), while others exhibited immediate flight, or rearing followed by flight (Fig. 2B; Table 1). The speed of the mouse movement was displayed in a heatmap (Fig. 2C), which reveals that all mice showed flight with a high speed before moving into the hut (light blue). Some of them dashed immediately after the looming stimulus, and others froze (pink color) or reared before the flight. These mice were acclimated 1 d before the looming experiments (10 min) and on the day of the experiments (10 min). However, if mice were acclimated only the day of looming experiments, the fear responses were not reliably elicited [10-loom (no accl.); Table 1]. Only 2/13 mice exhibited flight and freeze to a 10-looming stimulus, but others showed either rearing or no response. To elicit the fear response consistently, we conducted 2-d acclimation and used the 10-time looming stimulus to examine the underlying cellular mechanism of the looming-evoked fear responses.

### Starburst amacrine cell ablation reduced fear responses

Cellular mechanisms of looming stimulus-evoked fear responses have not been fully understood. Because a moving dark spot evoked the fear responses, the OFF channel of direction-selective ganglion cells (DSGCs) in the retina is likely to be involved (Yilmaz and Meister, 2013). Our data indicated that a dark moving edge, either looming or white-receding, evoked the freeze and flight responses (Fig. 1). Therefore, we examined whether the motion-detection pathway is involved in causing the fear responses by ablating retinal starburst amacrine cells (SACs), critical neurons for the retinal direction-selective pathway.

We generated a mouse line crossing ChAT-cre and diphtheria toxin receptor (DTR)-expressing lines and injected a dose of DT (3.2 or 10 ng) to exclusively ablate SACs in the retina (Hillier et al., 2017; Care et al., 2019; Kim et al., 2020). We first examined the effect of DT injection on the retinal neurons by injecting DT in one eye, and leaving another eye intact. We labeled SACs using an anti-ChAT-antibody, and labeled all retinal neurons with DAPI. In control eyes without DT injection, ON SACs were

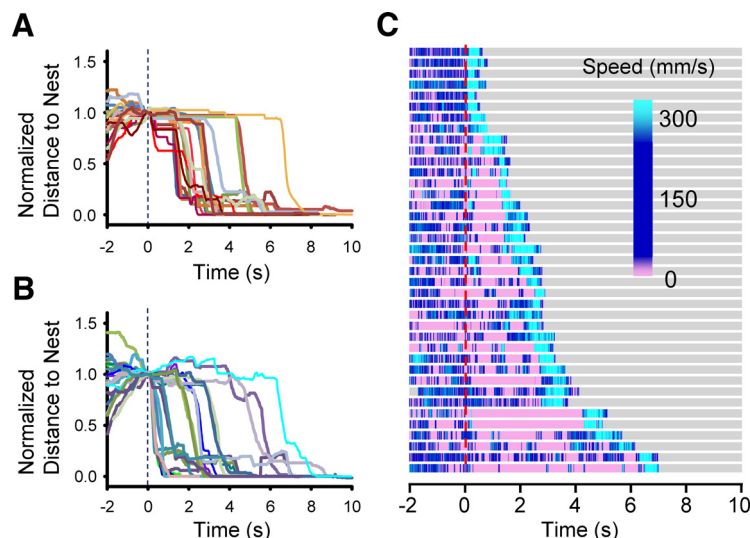


**Figure 2.** C57 wild-type mice exposed to the 10-looming stimulus. **A**, A group of mice froze before the flight response, indicated by straight lines after the stimulus (18/39 mice). **B**, Another group of mice exhibited immediate flight or rearing and flight responses (21/39 mice). **C**, A heatmap summary of mouse speed before and after 10-looming stimuli. A red dashed line indicates the onset of the looming stimulus. A high speed (light blue) at the end shows the flight response before moving into a hut. A low speed (pink) for  $>1$  s indicates the freeze response. Tracking was ended after mice moved into the hut.

labeled in the ganglion cell layer (GCL; Fig. 3*A*, *I*) at a density of  $1122 \pm 95$  cells/mm<sup>2</sup> ( $n=3$  eyes). In eyes with DT injection (Fig. 3*A*, *II*), ON SACs were reduced to  $389 \pm 151$  cells/mm<sup>2</sup> ( $n=4$  eyes,  $p=0.01$  vs control eyes, unpaired  $t$  test). Remaining SACs showed normal dendritic morphology and proper placement in the IPL (data not shown). In contrast, DAPI staining did not show differences between control and DT-injected eyes in the GCL ( $n=4$  eyes each, Control:  $10\,522 \pm 836$ , DT:  $10\,393 \pm 974$  cells/mm<sup>2</sup>,  $p=0.9$  unpaired  $t$  test). Similar results were obtained during the time period between 6 and 10 d after the initial DT injection. The average densities of DAPI stained neurons in the GCL in control and toxin-treated samples were similar to previous observations (Jeon et al., 1998). Therefore, we concluded that the protocol we used effectively and exclusively ablated SACs.

Because DT would be administrated by intraocular injection (Materials and Methods), we also tested whether the injection itself would disrupt the retinal neurons. We injected saline to the intraocular space of the ChAT-cre x DTR mice ( $n=5$  mice, 10 eyes). The number of ON SACs and DAPI-stained cells in the GCL did not change compared with noninjected eyes (DAPI:  $9903 \pm 173$  cells/mm<sup>2</sup>,  $p=0.52$ ; ON SACs:  $1184 \pm 41$  cells/mm<sup>2</sup>,  $p=0.51$ , unpaired  $t$  test), confirming that the intraocular injection did not affect the retinal neurons other than SACs.

Then, we examined the behavior of the ChAT-cre x DTR mice in response to the 10-time looming stimulus before and after the DT injection. Before the DT injection, 54 ChAT-cre x DTR mice exhibited similar fear responses to C57 wild-type mice. All the mutant mice exhibited fear responses: flight, freeze, or both (Fig. 3*B*; Table 2). The flight behavior was observed after a freeze or rearing in some mice (Fig. 3*B*, pink followed by light blue). In addition, four mice showed only a freeze response to the looming

stimulus (Fig. 3*B*, bottom four mice). The fear response was evoked by a looming stimulus of either 2–50° expansion (no mark) or 2–9° expansion (asterisk). The saline intraocular injection did not change the fear response. All of the saline-injected mice exhibited flight behavior, which was preceded by freeze or rearing in some mice (Table 2; Fig. 3*C*).

The DT intraocular injection changed the looming-evoked responses in half of the mutant mice. We divided them into two groups: fear response preserved (Group 1) and fear response disappeared (Group 2). Although DT was injected, the Group 1 mice still showed a fear response similar to the preinjected mice: flight, freeze, or both (Fig. 3*D*; Table 2). Some mice exhibited the freeze or rearing followed by flight, and four mice showed only a freeze response. In contrast, the Group 2 mice did not show either flight or freeze, but rearing was observed in 39% of mice (Fig. 3*E*; Table 2). The rest of the mice did not respond to the looming stimulus.

We initially injected 3.2 ng of DT per eye, and observed that a subset of mice exhibited no looming-evoked fear responses (Group 2;  $n=23$ ), but others exhibited the fear responses (Group 1;  $n=26$ ). Then, we increased the DT dose to 10 ng per eye, and all mice were categorized as Group 2. These mice exhibited a defensive response to the looming stimulus before the DT injection, which was eliminated by DT-mediated ablation of ON and OFF-SACs (Table 2; Fig. 3*E*). Because a previous publication failed to observe the SAC's contribution to the looming behavior (Wang et al., 2021), we used the same looming stimulus (2–9° expansion, ours was primarily 2–50°) to examine whether the stimulus difference induced the different outcomes. The smaller looming stimulus still evoked the fear responses before the DT injection (Fig. 3*B*, asterisks) but the DT injection removed those responses (Fig. 3*E*, asterisks).

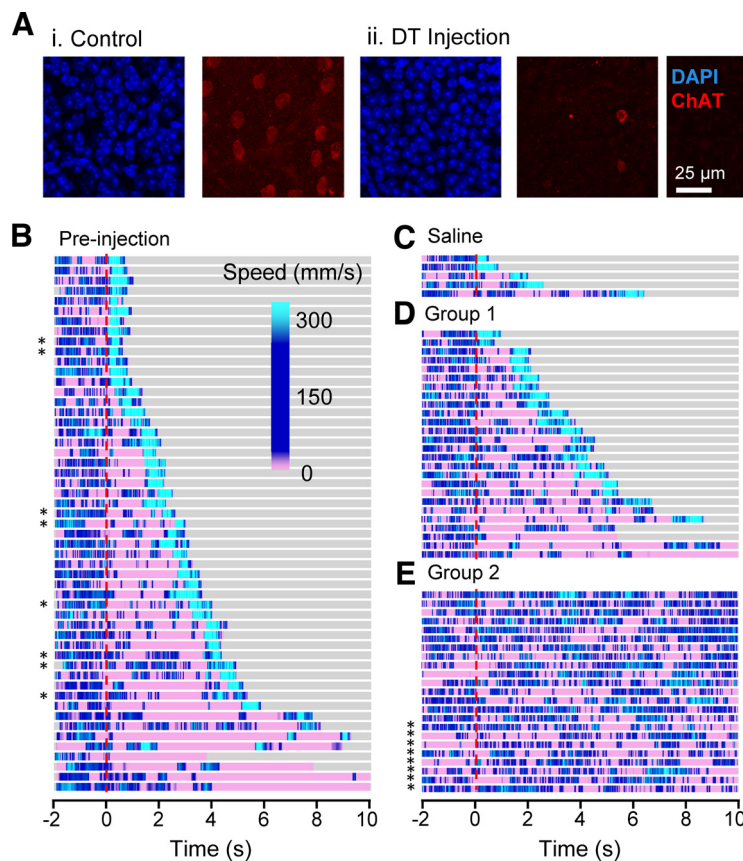


**Figure 3.** DT injection reduced the number of SACs and removed the looming-evoked fear responses. **A**, Using immunohistochemistry, (i) control and (ii) DT-injected retinas were labeled with DAPI and ChAT-antibody. There was no difference in the density of GCL layer cells between the control and injected groups. In contrast, the SAC density showed a significant reduction. **B**, Speed heatmap for mouse responses to the 10-time looming stimulus before DT injection. After the looming stimuli, mice displayed a combination of flight (high speed, light blue) and freezing (low speed, pink) responses. A red line indicates the onset of looming stimulus. Asterisks (\*) indicate that mice were exposed to the 2° to 9° looming stimulus. All other mice were exposed to the looming stimulus of 2° to 50°. **C**, Saline-injected mice showed flight responses to looming stimulus. **D**, Group 1 mice exhibited freeze and/or flight responses after DT injection. **E**, Group 2 mice did not show freeze and/or flight responses after DT injection.

In addition to looking for looming-evoked fear responses, we examined other visual behaviors to determine that these mice maintained otherwise functional vision. Mice that developed cataracts or corneal opacity at the time of behavior testing were removed from further analysis. In all DT-injected mice, we observed normal pupillary light reflexes. Furthermore, we conducted the SLAG test to examine mouse vision (Gil-Pages et al., 2013). All the mice that we tested before and after DT injection showed a positive SLAG test response ( $n = 12$  for pre-DT,  $n = 11$  for Group 1,  $n = 14$  for Group 2), demonstrated by their ability to both perceive and locate the wire cage during grasping. These experiments and observations

indicate that the DT-injected mice, both Groups 1 and 2, had functional vision. However, approximately half of them did not exhibit visually-evoked fear responses to the looming stimulus after the DT injection.

### Optomotor response and cellular examinations

The optokinetic response (OKR) disappears if SACs are eliminated (Yoshida et al., 2001), thus, measuring the OKR might indicate whether SACs were deleted by the DT injection. Because OKR is equivalent to the optomotor response (OMR) which can be conducted relatively easy in the lab (Douglas et al., 2005; Kretschmer et al., 2017), we measured the OMR from 29 preinjected mice,

**Table 2: The behavioral responses to 10-time looming before and after saline and DT injections in CHAT-DTR mice**

|              | Mouse number | Flight   | Freeze   | Rearing | No response |
|--------------|--------------|----------|----------|---------|-------------|
| Preinjection | 54           | 50 (93%) | 29 (54%) | 9 (17%) | 0           |
| Saline       | 5            | 5 (100%) | 1 (20%)  | 1 (20%) | 0           |
| Group 1      | 26           | 22 (85%) | 14 (54%) | 9 (35%) | 0           |
| Group 2      | 23           | 0        | 0        | 9 (39%) | 14 (61%)    |

Some mice showed multiple responses to a stimulus, such as freezing followed by flight, and the totals exceed 100%.

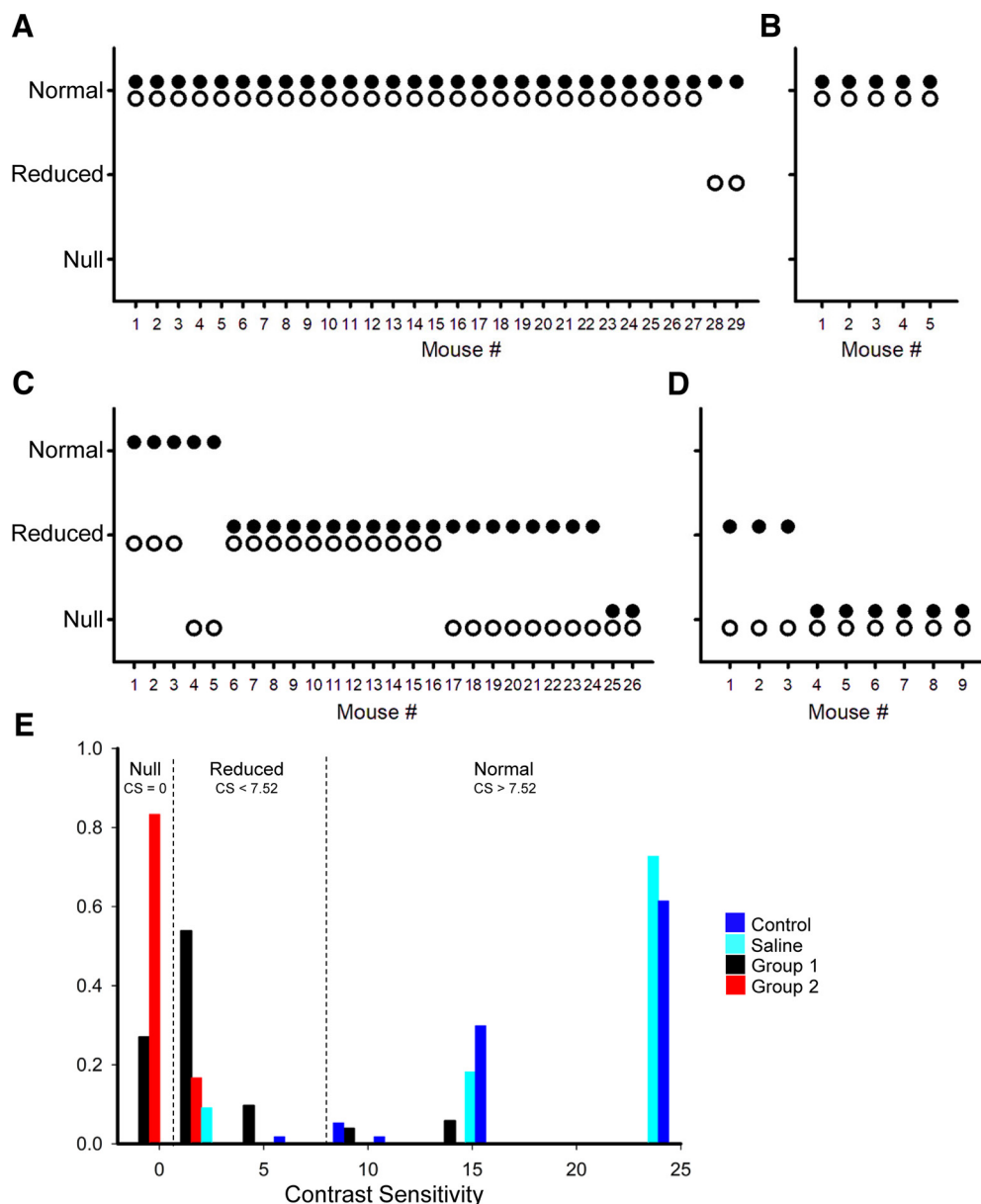


**Figure 4.** Optomotor responses (OMRs) before and after the DT injection. The black and white dots in **A–D** refer to one of the two eyes for each mouse. **A**, Before the DT injection, the OMR was measured. The average contrast sensitivity was 19.1 and the SD was 5.8. When the eye exhibited within the 2 SD, it was categorized as normal. If the sensitivity was lower than 2 SD, it was categorized as reduced. If the OMR was not recognized, it was categorized as null. Most eyes before the DT injection showed normal contrast sensitivity. **B**, Saline was injected into five mice, which all exhibited normal sensitivity. **C**, Group 1 mice exhibited reduced or null OMRs after one week of DT intravitreal injection. For those mice, the OMR sensitivity was reduced at least one of eyes. **D**, Group 2 mice exhibited reduced or null OMRs. These mice did not show the fear response after the DT intravitreal injection. **E**, A bar graph showing the distribution of the contrast sensitivities for each group. The frequency was normalized to each group and is shown as the proportion of eyes with the same contrast sensitivity value per group. The contrast sensitivity values are color coded: preinjection mice (blue), saline-injected mice (cyan), Group 1 DT-injected mice (black), and Group 2 DT-injected mice (red).

which showed an average contrast sensitivity of  $19.1 \pm 5.8$  (mean  $\pm$  SD). Each eye was characterized as either normal sensitivity (within 2 SD range:  $>7.5$ ), reduced sensitivity ( $<7.5$ ), or null OMR (no response to OMR stimulus; Fig. 4E). The preinjection mice exhibited normal OMR except for two eyes (Fig. 4A). The saline-injected mice similarly showed normal OMR (Fig. 4B).

The Group 1 DT-injected mice exhibited reduced OMR, indicating the decreased number of SACs (Fig. 4C). Some eyes even lost the OMR; however, the looming-evoked fear response still occurred. The Group 2 mice also exhibited reduced or null OMRs (Fig. 4D). These mice did not show the fear response to the looming stimulus. The OMR reduced or disappeared in both mouse groups (Fig. 4E) and no obvious distinction was recognized between



**Table 3: The number of cells in the GCL and SACs after saline and DT injections**

|         | Number of eyes | DAPI (GCL) (cells/mm <sup>2</sup> ) | ON SAC (cells/mm <sup>2</sup> ) | OFF SAC (cells/mm <sup>2</sup> ) |
|---------|----------------|-------------------------------------|---------------------------------|----------------------------------|
| Saline  | 10             | 9825 ± 275                          | 1184 ± 41                       | 1244 ± 33                        |
| Group 1 | 29             | 9762 ± 227                          | 166 ± 37*                       | 555 ± 62*                        |
| Group 2 | 26             | 9162 ± 303                          | 3 ± 1*#                         | 9 ± 4*#                          |

Values are mean ± SEM. Statistical differences are described in text. \*denotes statistical significance compared with the saline group, and #denotes statistical significance compared with Group 1.

them, suggesting that OMR is not an indicator for the looming-evoked fear responses.

To examine how surviving SACs that remain after DT injection may explain the persistence of visually-evoked fear responses, we performed immunohistochemistry on 55 retinas from 32 mice. DT-injected mice were euthanized for immunohistochemistry within 24 h after the behavioral examinations were conducted. Initially, we counted the DAPI-expressing cells in the GCL, which should include all ganglion cells and displaced amacrine cells. Based on remaining visual behaviors and lack of Cre-induced DTR expression, we expected that these neuronal populations would be unaffected by DT injection. This was supported by the number of DAPI-expressing cells, which was not different among the three mouse groups: saline-injected, Group 1, and Group 2 ( $p = 0.19$ , one-way ANOVA; Table 3; Fig. 5A). This indicated that the two doses of DT concentrations we used did not affect neural populations other than SACs.

Then, we counted ON and OFF SACs both in Groups 1 and 2 mice. The number of ON SACs was significantly reduced both in Groups 1 and 2 mice compared with saline-injected mice (Table 3;  $p = 10^{-17}$  for Group 1 and  $p = 10^{-10}$  for Group 2 vs control eyes, unpaired  $t$  test). In Group 1 mice, the average ON SACs were higher than those in Group 2 mice; however, some mice showed 0–1% of the normal cell density, and still exhibited the looming-evoked fear response (Fig. 3). The reduced-ON SACs explain the reduced OMR in Figure 4C,D (Joly et al., 2014). OFF SACs were also significantly reduced compared with the saline-injected eyes (Table 3); however, there was a difference between two groups; OFF-SACs in Group 1 were reduced by approximately half and preserved relatively normal dendritic structures (Fig. 5B), whereas OFF-SACs in Group 2 mice were reduced to ~1%. The number of remaining OFF SACs was significantly different between two groups ( $p = 10^{-9}$  Group 2 vs Group 1, unpaired test). ON SACs appeared to be more effectively ablated than OFF SACs (Fig. 5B–E), most likely attributable to the difficulty of DT penetration to the INL compared with the GCL from the intravitreal injection site. Because the looming-evoked fear response disappeared in the Group 2 mice, these results suggest that OFF SACs contribute to the initiation of fear responses.

We further examined the relation between OMR and the SAC numbers using a subset of Group 1 mice ( $n = 21$  eyes; Fig. 5F). As stated in the previous section, ON SACs were reduced in these mice but OFF SACs were still preserved. Some eyes showed OMR within the normal range and reduced range (Fig. 5F, red and blue lines). Five eyes showed no OMR, of which ON SACs were reduced to  $55 \pm 25$  cells/mm<sup>2</sup> (range 20–153, ~5% of the normal density), whereas the density of OFF SACs was  $243 \pm 42$  cells/mm<sup>2</sup> (20% of the normal density) and the looming

stimulus evoked freeze or flight responses. In contrast, the OFF-SAC density was reduced to ~1% in Group 2 mice (Table 3), with ON-SAC density being similar to the ~5% remaining ON-SAC population in Group 1, which did not show a fear response to the looming stimulus. Taken together, these results indicate that OFF SACs are required for the looming-evoked fear response.

## Discussion

In the present study, we found that the fear responses, flight and freeze, were consistently evoked by a 10-time looming stimulus with 2-d acclimation. We examined whether SACs were involved in the neural pathway for looming-evoked fear responses by injecting DT into the intravitreal space to ablate those cells. The fear responses disappeared in approximately half the DT injected mice. The reduced OMR did not correlate with the disappearance of the fear responses, and ON-SACs were effectively ablated by DT-injection. This suggests that the contribution of ON SACs to looming is low, but does not directly rule out the possibility of their involvement. The immunohistochemistry data revealed that mice with a considerable number of surviving OFF SACs maintained fear-evoked responses, whereas the fear response disappeared from mice where OFF SACs were almost entirely eliminated by DT. These results indicate that OFF SACs and downstream neurons, including the motion detection pathway, are critical for looming-evoked fear responses.

## Looming activating pathway in the CNS

The looming stimulus evokes freeze and flight responses, which serve to defend mice from a perceived threat. Threats can be categorized as imminent in the form of circa-strike and postencounter with an anticipation of a possible nociceptive event (Mobbs et al., 2009). The circa-strike is characterized by a direct predator attack, which may evoke panic behaviors in prey. In contrast, postencounter is defined as higher-level processing involving monitoring and predicting the outcome with a slower time course. The looming and sweeping stimuli mimic the imminent threat and postencounter, respectively.

Activity loci have been investigated in the human brain using the electroencephalogram (EEG) and fMRI. Imminent threats increase activity in the midbrain, including the periaqueductal gray (PAG), whereas postencounter threats activate the forebrain, hippocampus, hypothalamus, and amygdala (Mobbs et al., 2009). Alternatively, connections among the amygdala, hypothalamus, and PAG receive threat signals and produce defensive behavior (Adolphs, 2013). The amygdala is a well-known center for fear, which is activated by a looming visual cue but

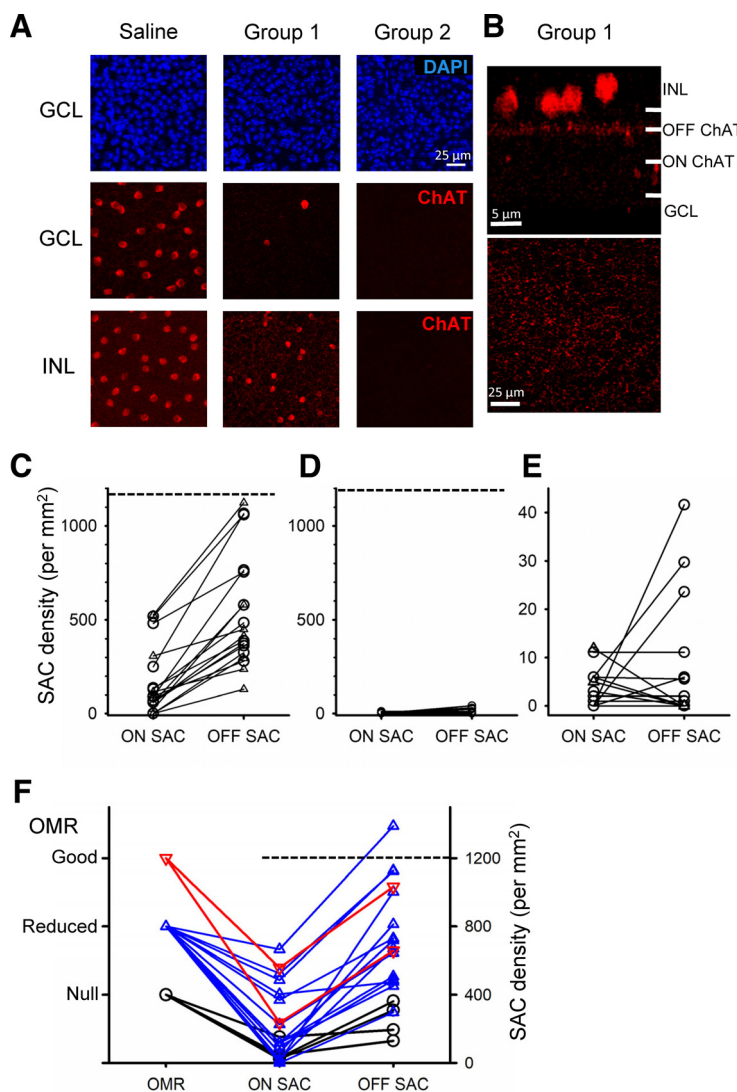


**Figure 5.** Immunohistochemical analysis of ON and OFF SACs after the DT injection. **A**, Saline-injected eyes exhibited normal densities of GCL-layer cells, and ON and OFF SACs in GCL and INL layers, respectively. The Group 1 mice showed significantly reduced ON SACs. OFF SACs were also reduced, but still remained. In contrast, ON and OFF SACs were significantly reduced in Group 2 mice. **B**, In Group 1 mice, the remaining OFF SACs exhibited normal dendritic structures. OFF ChAT band (side view) and dendritic network (top view) are shown. **C**, ON and OFF SAC density in Group 1 mice. The dotted line indicates the normal density. **D**, ON and OFF SAC density in Group 2 mice. The scale is same as the graph **C**. **E**, The same graph as **D**; however, the scale was adjusted. **F**, OMR and the densities of ON and OFF SACs were compared in twenty-one eyes from Group 1 mice. The red lines are mice that had normal OMR, blue lines are mice with reduced OMR, and black lines are mice with null OMR. Although ON SAC density was significantly decreased, some eyes exhibited OMR in normal and reduced ranges. The null-OMR mice exhibited the low ON SAC density. However, OFF SACs were relatively preserved (>20% of normal density).

not by a receding stimulus (Cappe et al., 2012). The amygdala responds strongly to frightened human faces and threatening animals, such as tarantulas, rather than neutral faces, animals, and objects (J. Yang et al., 2012). The PAG in the midbrain is also sensitive to approaching threats compared with receding threats or neutral objects (Coker-Appiah et al., 2013).

The neural pathway to the amygdala on detection of the looming visual stimulus has been investigated using mouse models. The parvalbumin-positive (PV<sup>+</sup>) excitatory neurons in the mouse superior colliculus (SC) are sensitive to the looming stimulus, which projects to the

parabigeminal nucleus (PBGN) and lateral posterior thalamic nucleus (LPTN), which relay inputs to the amygdala (Shang et al., 2015, 2018; Wei et al., 2015). Interestingly, PV<sup>+</sup> neuron projection through the PBGN evokes flight and freeze, whereas the neurons projecting through the LPTN induce only freezing behavior (Shang et al., 2018). A recent study revealed another critical projection from the mouse SC to the amygdala. A neural projection from SC to the ventral tegmental area in the midbrain, then to the central nucleus of the amygdala, is crucial for looming stimulus-evoked flight behavior (Zhou et al., 2019). It has not been fully understood how these separate pathways

control looming-evoked behavior. However, multiple investigations assured that the looming stimulus activates the neural projection from SC to the amygdala that evokes fear responses.

### Looming-evoked pathway in the retina

It is certain that the looming stimulus activates retinal neurons before the SC and amygdala. However, we have just begun to examine the retinal neural pathway for looming detection. In the fly eyes, the lobula plate/lobula columnar, Type II (LPLC2) neuron has been identified as an ultrasensitive looming detector (Klapoetke et al., 2017). The lobula plate is analogous to the vertebrate colliculus (Sanes and Zipursky, 2010), and the LPLC2 cells are neurons distinct from directionally-selective cells. These cells strongly respond to a looming stimulus, but weakly to a moving stimulus in a lateral direction. Similarly, the lobula giant movement detector (LGMD) and its downstream neurons are designated looming detectors in the locust eyes (Gabbiani et al., 2002; Guest and Gray, 2006).

In the mouse retina, a large number of ganglion and amacrine cell types have been recently reported (Baden et al., 2016; Yan et al., 2020). Because these cells encode image features, there might be a looming detector similar to the fly and locust eyes. Alternatively, multiple types of direction-selective cells, which respond to specific directions of motion, may detect the looming stimulus, which activates the SC-amygdala pathway to evoke fear responses.

Yilmaz and Meister (2013) predicted that the looming behavior is induced by a transient OFF channel, such as the PV-5 cells, ON-OFF direction-selective ganglion cells (DSGCs), and W-3 cells. Münch et al. (2009) examined the looming stimulus-evoked responses in PV-5 cells, which are OFF-responding, large ganglion cells. They strongly responded to an approaching motion, suggesting that these are the looming detector. However, unlike the looming detector in the insect eyes, the receptive field of PV-5 cells was not large. Also, behavioral testing has not been conducted with PV-5 cell-disrupted mice. PV-5 cells are potentially the same as the transient OFF- $\alpha$  ganglion cells in the next paragraph (Farrow et al., 2013), and it is inconclusive whether the PV-5 cells are the looming detector in the mouse retina.

Kim et al. (2020) recently reported that the vGluT3 amacrine cells are the looming detector. vGluT3 cells are a unique type of amacrine cell, which release glutamate as a neurotransmitter onto W-3 and OFF- $\alpha$  ganglion cells (Lee et al., 2014, 2016). When the vGluT3 cells transiently responded to a looming stimulus, the W-3 ganglion cells similarly responded in a transient fashion, and the OFF- $\alpha$  ganglion cells exhibited an increasing response depending on the stimulus expansion speed. This result indicates that the W-3 ganglion cells code the onset of the looming stimulus, while the OFF- $\alpha$  cells encode the speed of expanding motion (Kim et al., 2020). Remarkably, when vGluT3 amacrine cells were removed by diphtheria toxin, the freezing response to a looming stimulus was significantly reduced. Therefore, vGluT3 amacrine cells serve as a looming detector. The involvement of the OFF-t  $\alpha$

ganglion cells in the looming response was confirmed by genetic methods by Wang et al. (2021).

We observed that fear responses were evoked by looming and white receding stimuli, but not by the flip screen, indicating that the moving dark edge is critical. Therefore, we targeted the SACs using diphtheria toxin (DT) for ablation, as SACs provide synaptic inputs to DSGCs and are crucial for motion detection in the retina (Yoshida et al., 2001). The DT injection did not always completely remove SACs, attributable to the conservative DT dose we injected. However, the varied SAC reductions and behavior outcomes offered a clue for the underlying cellular mechanism. When the DT ablated primarily ON SACs, we observed the reduced OMR; however, the looming-evoked fear responses still occurred (Group 1). When both ON and OFF SACs were eliminated, the fear responses were also removed (Group 2). The number of DAPI-stained GCL cells did not change in both groups, indicating that other neurons were not affected by the DT injection. While we cannot directly rule out there being any impact from ON SACs, these results indicate that OFF SACs and downstream direction-selective ganglion cells (DSGCs) are crucial for looming visual stimuli-evoked flight.

How do our results complement the results of Kim et al. (2020) and Wang et al. (2021)? The SAC-DSGC and vGluT3-W3/off- $\alpha$  connections are two separate neural pathways in the retina. Both SACs and vGluT3 are amacrine cells, and there are no synaptic connections among them (Lee et al., 2014). Kim et al. (2020) found that the vGluT3 removal suppressed the freeze response to the looming stimulus. In contrast, we found that the SAC disruption eliminated both flight and freeze responses. Potentially, two separate retinal circuits mediate different aspects of looming behavior, similar to the multiple SC-amygdala pathways (Shang et al., 2018). Alternatively, two separate pathways may coordinate to sense looming and generate a fear response. The W-3 ganglion cells possess a large antagonistic surround region and sense local motion (Kim and Kerschensteiner, 2017). ON-OFF DSGCs sense high-speed motion (Sivyer et al., 2010). When one of them is disrupted, mice may no longer respond to a looming stimulus.

Wang et al. (2021) examined the effect of SAC ablation using the same methods we did, but did not observe the reduced looming-triggered defensive response. We postulated a couple of factors led to the different outcomes: stimulus size and SAC density. We matched their looming stimulus by changing the expansion to 9° instead of the 50° we used. However, the DT injection in our mice removed the defensive response, indicating that stimulus differences may not be the reason for the different looming responses. Another possibility is that they showed reduced density of SAC in their supplement figure but were not clear about the ON versus OFF SACs. In case they only examined ON SACs, OFF SACs might still have existed and induce the defensive response, similar to our Group 1 mice.

In conclusion, we found that OFF SACs and downstream pathways are crucial for looming detection and driving optically-derived fear responses. However, because we could



not eliminate ON and OFF SACs separately, potential contribution of ON SACs to the looming response cannot be ruled out. Multiple neural pathways in the retina might be critical to inducing the defensive response to an approaching shadow. We believe that our study has revealed a link between early visual processing in the retina by a specific cell type and visual cue-evoked behavioral outcomes.

## References

- Adolphs R (2013) The biology of fear. *Curr Biol* 23:R79–R93.
- Baden T, Berens P, Franke K, Román Rosón M, Bethge M, Euler T (2016) The functional diversity of retinal ganglion cells in the mouse. *Nature* 529:345–350.
- Bertels J, Bourguignon M, de Heering A, Chetail F, De Tiège X, Cleeremans A, Destrebecqz A (2020) Snakes elicit specific neural responses in the human infant brain. *Sci Rep* 10:7443.
- Blanchard DC, Hynd AL, Minke KA, Minemoto T, Blanchard RJ (2001) Human defensive behaviors to threat scenarios show parallels to fear- and anxiety-related defense patterns of non-human mammals. *Neurosci Biobehav Rev* 25:761–770.
- Cappe C, Thelen A, Romei V, Thut G, Murray MM (2012) Looming signals reveal synergistic principles of multisensory integration. *J Neurosci* 32:1171–1182.
- Care RA, Kastner DB, De la Huerta I, Pan S, Khoche A, Della Santina L, Gamlin C, Santo Tomas C, Ngo J, Chen A, Kuo YM, Ou Y, Dunn FA (2019) Partial cone loss triggers synapse-specific remodeling and spatial receptive field rearrangements in a mature retinal circuit. *Cell Rep* 27:2171–2183.e5.
- Coker-Appiah DS, White SF, Clanton R, Yang J, Martin A, Blair RJ (2013) Looming animate and inanimate threats: the response of the amygdala and periaqueductal gray. *Soc Neurosci* 8:621–630.
- De Franceschi G, Vivattanasarn T, Saleem AB, Solomon SG (2016) Vision guides selection of freeze or flight defense strategies in mice. *Curr Biol* 26:2150–2154.
- Douglas RM, Alam NM, Silver BD, McGill TJ, Tschetter WW, Prusky GT (2005) Independent visual threshold measurements in the two eyes of freely moving rats and mice using a virtual-reality optokinetic system. *Vis Neurosci* 22:677–684.
- Euler T, Detwiler PB, Denk W (2002) Directionally selective calcium signals in dendrites of starburst amacrine cells. *Nature* 418:845–852.
- Euler T, Haverkamp S, Schubert T, Baden T (2014) Retinal bipolar cells: elementary building blocks of vision. *Nat Rev Neurosci* 15:507–519.
- Farrow K, Teixeira M, Szikra T, Viney TJ, Balint K, Yonehara K, Roska B (2013) Ambient illumination toggles a neuronal circuit switch in the retina and visual perception at cone threshold. *Neuron* 78:325–338.
- Farshi P, Fyk-Kolodziej B, Krolewski DM, Walker PD, Ichinose T (2016) Dopamine D1 receptor expression is bipolar cell type-specific in the mouse retina. *J Comp Neurol* 524:2059–2079.
- Gabbiani F, Krapp HG, Koch C, Laurent G (2002) Multiplicative computation in a visual neuron sensitive to looming. *Nature* 420:320–324.
- Gil-Pages M, Stiles RJ, Parks CA, Neier SC, Radulovic M, Oliveros A, Ferrer A, Reed BK, Wilton KM, Schrum AG (2013) Slow angled-descent forepaw grasping (SLAG): an innate behavioral task for identification of individual experimental mice possessing functional vision. *Behav Brain Funct* 9:35.
- Guest BB, Gray JR (2006) Responses of a looming-sensitive neuron to compound and paired object approaches. *J Neurophysiol* 95:1428–1441.
- Hillier D, Fiscella M, Drinnenberg A, Trenholm S, Rompani SB, Raics Z, Katona G, Juettner J, Hierlemann A, Rozsa B, Roska B (2017) Causal evidence for retina-dependent and -independent visual motion computations in mouse cortex. *Nat Neurosci* 20:960–968.
- Ichinose T, Hellmer CB (2016) Differential signalling and glutamate receptor compositions in the OFF bipolar cell types in the mouse retina. *J Physiol* 594:883–894.
- Ichinose T, Fyk-Kolodziej B, Cohn J (2014) Roles of ON cone bipolar cell subtypes in temporal coding in the mouse retina. *J Neurosci* 34:8761–8771.
- Jeon CJ, Strettoi E, Masland RH (1998) The major cell populations of the mouse retina. *J Neurosci* 18:8936–8946.
- Joly S, Guzik-Kornacka A, Schwab ME, Pernet V (2014) New mouse retinal stroke model reveals direction-selective circuit damage linked to permanent optokinetic response loss. *Invest Ophthalmol Vis Sci* 55:4476–4489.
- Kim T, Kerschensteiner D (2017) Inhibitory control of feature selectivity in an object motion sensitive circuit of the retina. *Cell Rep* 19:1343–1350.
- Kim T, Shen N, Hsiang JC, Johnson KP, Kerschensteiner D (2020) Dendritic and parallel processing of visual threats in the retina control defensive responses. *Sci Adv* 6:eabc9920.
- Klapoetke NC, Nern A, Peek MY, Rogers EM, Breads P, Rubin GM, Reiser MB, Card GM (2017) Ultra-selective looming detection from radial motion opponency. *Nature* 551:237–241.
- Koehler CC, Hall LM, Hellmer CB, Ichinose T (2019) Using looming visual stimuli to evaluate mouse vision. *J Vis Exp* (148):10.3791/59766.
- Kretschmer F, Tariq M, Chatila W, Wu B, Badea TC (2017) Comparison of optomotor and optokinetic reflexes in mice. *J Neurophysiol* 118:300–316.
- Lee S, Chen L, Chen M, Ye M, Seal RP, Zhou ZJ (2014) An unconventional glutamatergic circuit in the retina formed by vGluT3 amacrine cells. *Neuron* 84:708–715.
- Lee S, Zhang Y, Chen M, Zhou ZJ (2016) Segregated glycine-glutamate co-transmission from vGluT3 amacrine cells to contrast-suppressed and contrast-enhanced retinal circuits. *Neuron* 90:27–34.
- Mobbs D, Marchant JL, Hassabis D, Seymour B, Tan G, Gray M, Petrovic P, Dolan RJ, Frith CD (2009) From threat to fear: the neural organization of defensive fear systems in humans. *J Neurosci* 29:12236–12243.
- Münch TA, da Silveira RA, Siegert S, Viney TJ, Awatramani GB, Roska B (2009) Approach sensitivity in the retina processed by a multifunctional neural circuit. *Nat Neurosci* 12:1308–1316.
- Prusky GT, Alam NM, Beekman S, Douglas RM (2004) Rapid quantification of adult and developing mouse spatial vision using a virtual optomotor system. *Invest Ophthalmol Vis Sci* 45:4611–4616.
- Ren C, Tao Q (2020) Neural circuits underlying innate fear. *Adv Exp Med Biol* 1284:1–7.
- Sanes JR, Zipursky SL (2010) Design principles of insect and vertebrate visual systems. *Neuron* 66:15–36.
- Schiff W, Caviness JA, Gibson JJ (1962) Persistent fear responses in rhesus monkeys to the optical stimulus of “looming.” *Science* 136:982–983.
- Schindelin J, Arganda-Carreras I, Frise E, Kaynig V, Longair M, Pietzsch T, Preibisch S, Rueden C, Saalfeld S, Schmid B, Tinevez JY, White DJ, Hartenstein V, Eliceiri K, Tomancak P, Cardona A (2012) Fiji: an open-source platform for biological-image analysis. *Nat Methods* 9:676–682.
- Shang C, Liu Z, Chen Z, Shi Y, Wang Q, Liu S, Li D, Cao P (2015) BRAIN CIRCUITS. A parvalbumin-positive excitatory visual pathway to trigger fear responses in mice. *Science* 348:1472–1477.
- Shang C, Chen Z, Liu A, Li Y, Zhang J, Qu B, Yan F, Zhang Y, Liu W, Liu Z, Guo X, Li D, Wang Y, Cao P (2018) Divergent midbrain circuits orchestrate escape and freezing responses to looming stimuli in mice. *Nat Commun* 9:1232.
- Shekhar K, Lapan SW, Whitney IE, Tran NM, Macosko EZ, Kowalczyk M, Adiconis X, Levin JZ, Nemesh J, Goldman M, McCarroll SA, Cepko CL, Regev A, Sanes JR (2016) Comprehensive classification of retinal bipolar neurons by single-cell transcriptomics. *Cell* 166:1308–1323.e1330.
- Sivyer B, van Wyk M, Vaney DI, Taylor WR (2010) Synaptic inputs and timing underlying the velocity tuning of direction-selective ganglion cells in rabbit retina. *J Physiol* 588:3243–3253.
- Temizer I, Donovan JC, Baier H, Semmelhack JL (2015) A visual pathway for looming-evoked escape in larval zebrafish. *Curr Biol* 25:1823–1834.



- Wang F, Li E, De L, Wu Q, Zhang Y (2021) OFF-transient alpha RGCs mediate looming triggered innate defensive response. *Curr Biol* 31:2263–2273 e2263.
- Wei P, Liu N, Zhang Z, Liu X, Tang Y, He X, Wu B, Zhou Z, Liu Y, Li J, Zhang Y, Zhou X, Xu L, Chen L, Bi G, Hu X, Xu F, Wang L (2015) Processing of visually evoked innate fear by a non-canonical thalamic pathway. *Na Commun* 6:6756.
- Yan W, Laboulaye MA, Tran NM, Whitney IE, Benhar I, Sanes JR (2020) Mouse retinal cell atlas: molecular identification of over sixty amacrine cell types. *J Neurosci* 40:5177–5195.
- Yang J, Bellgowan PS, Martin A (2012) Threat, domain-specificity and the human amygdala. *Neuropsychologia* 50:2566–2572.
- Yang X, Liu Q, Zhong J, Song R, Zhang L, Wang L (2020) A simple threat-detection strategy in mice. *BMC Biol* 18:93.
- Yilmaz M, Meister M (2013) Rapid innate defensive responses of mice to looming visual stimuli. *Curr Biol* 23:2011–2015.
- Yoshida K, Watanabe D, Ishikane H, Tachibana M, Pastan I, Nakanishi S (2001) A key role of starburst amacrine cells in originating retinal directional selectivity and optokinetic eye movement. *Neuron* 30:771–780.
- Zhou Z, Liu X, Chen S, Zhang Z, Liu Y, Montardy Q, Tang Y, Wei P, Liu N, Li L, Song R, Lai J, He X, Chen C, Bi G, Feng G, Xu F, Wang L (2019) A VTA GABAergic neural circuit mediates visually evoked innate defensive responses. *Neuron* 103:473–488.e6.